HYBRID SHARING FOR MULTI-LABEL IMAGE CLASSIFICATION

Zihao Yin[2,3], **Chen Gan**[2,3], **Kelei He**[1,3]*, **Yang Gao**[2,3] and **Junfeng Zhang**[1,3]
[1] Medical School of Nanjing University
[2] State Key Laboratory for Novel Software Technology, Nanjing University
[3] National Institute of Healthcare Data Science, Nanjing University
{zihao.yin, chengan}@smail.nju.edu.cn
{hkl, gaoy, jfzhang}@nju.edu.cn

ABSTRACT

Existing multi-label classification methods have long suffered from label heterogeneity, where learning a label obscures another. By modeling multi-label classification as a multi-task problem, this issue can be regarded as a negative transfer, which indicates challenges to achieve simultaneously satisfied performance across multiple tasks. In this work, we propose the Hybrid Sharing Query (HSQ), a transformer-based model that introduces the mixture-of-experts architecture to image multi-label classification. HSQ is designed to leverage label correlations while mitigating heterogeneity effectively. To this end, HSQ is incorporated with a fusion expert framework that enables it to optimally combine the strengths of task-specialized experts with shared experts, ultimately enhancing multi-label classification performance across most labels. Extensive experiments are conducted on two benchmark datasets, with the results demonstrating that the proposed method achieves state-of-the-art performance and yields simultaneous improvements across most labels. The code is available at this URL.

1 INTRODUCTION

In computer vision, multi-label classification (MLC) attempts to predict multiple labels that may simultaneously appear in a single sample. It is more realistic and intuitive as a sample typically has multiple attributes in real scenarios. However, the semantic correlation and heterogeneity among different labels pose a significant challenge to MLC, resulting in the labels either complement or conflict with each other. Previous works (Liu et al., 2021a; Ridnik et al., 2023; Ye et al., 2020) achieved impressive performance via transformers or graph neural networks, trying to explore the correlation among labels with shared backbone across labels. These approaches neglected the heterogeneity among labels, which becomes the key obstacle to simultaneous improvement across labels.

In contrast to traditional multi-label classification approaches, MLC can be formulated as a multi-task learning (MTL) problem by modeling the prediction of each label as an individual task. The correlation and heterogeneity of the labels in MLC thus correspond to the task transfer problem of MTL, where learning a new task may perfect (positive transfer) or deteriorate (negative transfer) another. Under this context, the power of MTL in mitigating negative transfer may help improve the performance of MLC.

Precedent works like (Ma et al., 2018) in MTL include a mixture of experts (MoE, (Jacobs et al., 1991)), which utilizes a group of learned experts to handle different tasks separately. MOE has been widely adopted in natural language processing, where experts are expected to process words of various lexical categories. We advocate employing MoE in MLC image classification, which shares commonality with lexical category handling. Furthermore, we notice that the conventional MoE approach has primarily emphasized the utilization of expert groups within a specific task, with limited attention to the exchange of expertise group knowledge across different tasks. This approach may not align seamlessly with the MLC requirements, which will be scrutinized in our work.

*: Corresponding author

In this work, we introduce Hybrid Sharing Query (HSQ), a MoE-based MLC method with a novel proposed fusion strategy to better exploit semantic correlation and heterogeneity among labels and generate better underlying shared representation and task-specific representation. Additionally, we prioritize the adaptive fusion of label-specific and shared features in the classification task of each label, suppressing negative transfer and enhancing performance on the majority of labels. Specifically, we employ a group of shared experts to mine correlation among labels to generate multiple distinct shared features while assigning a group of task-specialized experts to each task to extract a series of label-specific features. This design can balance label-specific and shared features across labels while also emphasizing unique label-specific features for each individual label. Moreover, we employ gate networks to adaptively re-weight and harmonize features from task-specialized experts and shared experts, enhancing positive correlations and suppressing negatives among tasks.

Experiments show that the proposed method outperforms all tested baselines across multiple datasets on the majority of labels. The proposed method is also compatible with transformer-based MLC methods, indicating potential improvement to existing works.

Our contribution is three-fold:

• We present MoE to the MLC task, with gated task-specialized and shared experts to capture correlation and heterogeneity adaptively by formulating the MLC as an MTL problem.

• We empirically demonstrate that the fused experts help to extract correlations between tasks, encourage positive correlation sharing and suppress negative transfer, which benefits the overall and per-label performance and mitigates cross-label performance gap.

• We verify the superiority of our proposed model on two benchmark datasets with state-of-the-art performance overall and per-label.

2 Related Work

Multi-label classification in computer vision. Models via various approaches have been proposed to address MLC. Zhu et al. (2017) use convolutional networks on an attention map to optimize ResNet prediction. Rajpurkar et al. (2017) solve the medical multi-label problem by using DenseNet (Huang et al., 2017). Wang et al. (2016) attempt to extract features from the image and generate the label as a sequence through a learned joint embedding space. Chen et al. (2019a) introduce graph convolutional network into this task, mapping label word embedding to inter-dependent object classifiers. Lanchantin et al. (2021a); Liu et al. (2021a) introduce transformer into MLC. These methods fail to see the negative transfer and positive correlation among labels. Some works also notice a similar problem in MLC from the MTL aspect. Wu et al. (2019) try to mitigate such a problem via a different architecture. Our study aims to improve overall performance in MLC while attempting to simultaneously enhance performance on as many labels as possible.

Multi-task learning. MLC can be recognized as a special case of MTL, treating each label as a separate classification task (Wu et al., 2019). Previous works on this topic include hard and soft parameter sharing, *etc*. Hard parameter sharing (Caruana, 1997) comes with a shared feature extraction backbone as a bottom and task-specialized towers as a top. Soft parameter sharing does not explicitly share network components across tasks but jointly learns other information through gradient sharing or other techniques. Duong et al. (2015); Yang and Hospedales (2017) encourage knowledge sharing across experts via different constraints like L2 norm. Cross-Stitch (Misra et al., 2016) trains two networks for two tasks and shares gradients between some layers controlled by gates. However, these architectures require more attention to the correlations among tasks, and the naive knowledge-sharing strategy may hamper the performance of models. In this work, we propose HSQ to reveal these correlations in the hope of generating a better representation for each task.

Mixture of experts in deep learning. Efforts have been made to improve models' performance by scaling up the model size with MoE (Jacobs et al., 1991), which first attempts to combine the outputs of several experts with a gate network. MMOE (Ma et al., 2018) with similar settings further decouples the seesaw phenomenon between several tasks by assigning exclusive gate and tower networks to each task. MOEC (Xie et al., 2023) adopts a clustering loss to impose variance-based constraints on the routing stage, obtaining clusters of experts with more diverse knowledge.

PLE (Tang et al., 2020) adds shared and task-specific experts to MMOE to allow better information sharing between tasks. Traditional MoE imposes a substantial computational burden since all experts activate, even when only some tasks are required. To mitigate such a cost, the sparse MoE (Shazeer et al., 2017) strategy emerges in contrast to the regular *dense* one. The routing strategy determines which experts contribute to the task output. Zhou et al. (2022); Rosenbaum et al. (2018); Nie et al. (2021); Zuo et al. (2022); Roller et al. (2021); Dai et al. (2022) and others explore various routing strategies, including randomizing, hashing, expert-choosing, *etc*. Switch Transformer (Fedus et al., 2022) introduces a sparse MoE to the transformer layer to replace the feed-forward neural network. Our method introduces the MoE into the multi-label classification field by virtue of task-specialized and shared experts exploiting correlations among tasks. Moreover, we utilize a gate network to enhance positive correlation and suppress negative correlation in pursuit of better fusion.

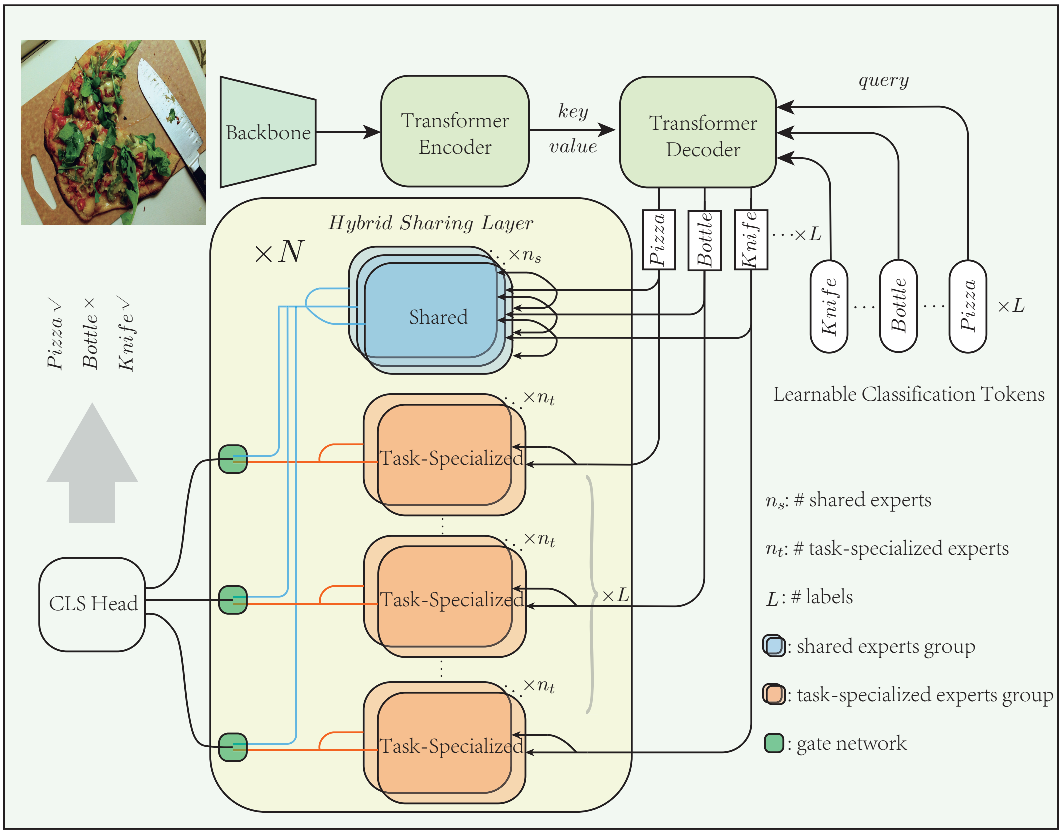

Figure 1: The architecture of the proposed HSQ. After being extracted by the backbone, the input image's features are then processed by a transformer, where learnable classification tokens are used as the query. N Hybrid Sharing Layers are employed sequentially, consisting of L groups of task-specialized experts and a group of shared ones. Individual gates for every group control the weighted outputs. A final classification head is utilized to make predictions.

3 METHOD

The MLC task for images is to find all possible correct labels in a pre-defined label set for a provided image. Thus, our model takes the provided image I and gives probability scoring $\hat{\mathcal{L}} \in \mathbb{R}^L$ on all labels $\mathcal{L}$. The proposed HSQ model comprises three main parts, namely, 1) feature extraction backbone, 2) query transformer, and 3) mixture-of-expert hybrid sharing head. The backbone extracts image representation with a robust replaceable network, followed by a transformer-based query model to explore underlying information between such extracted representation and each given label. The Hybrid Sharing Layers are applied to better exploit the correlations between every possible task and suppress potential negative transfer problems.

3.1 Feature extraction backbone

Features in any given image will be extracted through a feature extraction backbone. Multiple preceding works have contributed to this stage. We employ various well-established models to capture global and local feature information within images more effectively. For a 3-channel input image $I \in \mathbb{R}^{3\times H_i\times\ W_i}$, H_i and W_i are the height and width of an image. A feature extractor is applied to extract feature $R \in \mathbb{R}^{C_i\times H\times W}$, where C_i denotes the number of feature embedding, with a succeeding convolutional layer linearly projecting its feature space from C_i into C.

3.2 Query transformer

The semantic heterogeneity across labels requires the model to discern and capture unique feature representations specific to each individual task. Inspired by the remarkable performance of the query-based classifier, we employ learnable query tokens for classification to mitigate semantic conflicts between tasks. Specifically, this work employs a transformer to better extract and wrap task-specific underlying features in class-wise learnable tokens.

Given an extracted image representation R, an encoder-decoder standard transformer is applied to inspect features for each label. On the encoder side, the image representation from the backbone is flattened into $R \in \mathbb{R}^{C\times HW}$ and proceeded by N_e encoder layers as tokens. To decouple different labels effectively, we endorse Liu et al. (2021a); Lanchantin et al. (2021b) to use learnable tokens as the query. On the decoder side, a learnable token is fed to the transformer decoder as the query for each possible label so that the feature of each label would be learned individually. N_d decoder layers are stacked to extract the features of input representations in accordance with each possible label. The decoder layer accepts $T \in \mathbb{R}^{L\times C}$ for every L possible label, where C is the embedding dimension for each token. The cross-attention module in the transformer decoder performs on the query from the learnable label tokens (decoder) and the key and value from the extracted features (encoder), facilitating each label to mine respective representations.

3.3 Hybrid Sharing Layer

Given the potential semantic correlations among different labels, the features extracted from corresponding tasks may exhibit a positive correlation, providing complementary information to enhance model performance. However, improper exploitation of these correlations through learning jointly may cause performance degeneration since parts of these labels conflict with each other semantically due to their inherent heterogeneity, making them hard to learn jointly. To better leverage the positive correlations while suppressing detrimental impact due to heterogeneity between different tasks, we introduce the MoE mechanism into the multi-label classification area, inspired by the success of Progressive Layered Extraction (PLE) (Tang et al., 2020). Particularly, we employ several shared and task-specialized experts to capture positively correlated features among tasks and task-specific features, respectively, with a gate network adaptively fusing these features. The design of experts and gates can be very flexible and compatible as long as the output shapes are aligned, and in this work, we employ simple but effective linear layers to illustrate our approach.

Figure 2 depicts the details of Hybrid Sharing Layers, where L indicates the number of tasks, *i.e.* the number of labels in multi-label classification. For any task $t_i, i \in \{1, 2, \cdots L\}$, a group of task-specialized experts $E_{t_i,j}, j \in \{1, 2, \cdots n_t\}$, is assigned to extract features for this task exclusively, where n_t refers to the number of experts for this task. Apart from these task-specialized experts groups for every task, a group of shared experts $E_{s,j}, j \in \{1, 2, \cdots n_s\}$ is responsible for gathering global patterns and dispatching them to those potentially positively correlated tasks. Outputs of each expert group are harmonized by gate network, respectively, so that each task would have customized control on the weight of task-specialized and shared experts' outputs.

Algorithm 1 outlines the detailed mechanism of the MoE mechanism that we applied. Let $X_t \in \mathbb{R}^{N\times L\times d_i}$ be a batched input to the mixture-of-expert layer, where N refers to batch size and d_i means input embedding dimension. And let X_s be the input for shared experts group with the exact same shape as X_t. The outputs of a Hybrid Sharing Layer comprise task-specialized outputs and a shared output.

In the task-specialized section, each label (task) is processed independently. For a batched input $X_{t_i} \in \mathbb{R}^{N\times d_i}$ on task t_i, a set of task-specific experts, denoted as $E_{t_i,j} \in \mathbb{R}^{d_i\times d_o}$, is utilized,

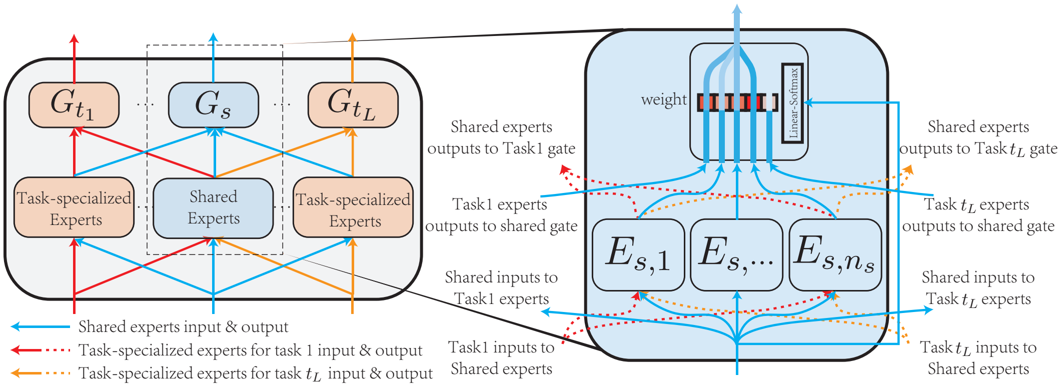

G_{t_1}
G_s
G_{t_L}
Task-specialized Experts
Shared Experts
Task-specialized Experts
Shared experts input & output
Task-specialized experts for task 1 input & output
Task-specialized experts for task t_L input & output
weight
Linear-Softmax
Shared experts outputs to Task1 gate
Shared experts outputs to Task t_L gate
Task1 experts outputs to shared gate
Task t_L experts outputs to shared gate
$E_{s,1}$
$E_{s,\dots}$
E_{s,n_s}
Shared inputs to Task1 experts
Shared inputs to Task t_L experts
Task1 inputs to Shared experts
Task t_L inputs to Shared experts

Figure 2: The Architecture of a Hybrid Sharing Layer. For L labels, the layer consists of L groups of task-specialized experts and a group of shared experts. The detailed structure of the shared experts is illustrated on the right.

where j represents the j-th expert in the group. $Y_{t_i|t_i,j} = X_{t_i}E_{t_i,j} \in \mathbb{R}^{N\times d_o}$ represents the output of expert $E_{t_i,j}$ on task t_i. The subscript of Y, separated by $|$, refers to the output task and expert subscript, respectively, meaning that it is the output of the j-th task-specialized expert in t_i and takes inputs from task t_i. Similarly, a group of shared experts, denoted as $E_{s,j} \in \mathbb{R}^{d_i\times d_o}$, is used for task t_i. Shared experts, which would be used in all tasks, also accept X_{t_i} in task t_i, and $Y_{t_i|s,j} = X_{t_i}E_{s,j} \in \mathbb{R}^{N\times d_o}$ represents the output of expert $E_{s,j}$ on task t_i. A gate network, denoted as $G_{t_i} \in \mathbb{R}^{d_i\times(L\cdot n_t+n_s)}$, is employed to produce weights for outputs from all shared and task-specialized experts on task t_i. The gate network takes X_{t_i} as input, and outputs $\mathrm{Softmax}(X_{t_i}G_{t_i}) \in \mathbb{R}^{N\times(n_t+n_s)}$ as the weights for experts' outputs. Here, n_t task-specialized experts for t_i and all n_s shared ones are employed. The task output is a weighted mean of all experts with activation σ, as described in the following equations, where (k) stands for tensor indexing.

$$\begin{aligned} Y_{t_i} &= \mathrm{Concat}(Y_{t_i|t_i,j}, Y_{t_i|s,j}) \in \mathbb{R}^{N\times d_o\times(n_t+n_s)} \\ O_{t_i} &= \sum_k \left[\sigma(Y_{t_i})^{(k)} \odot \mathrm{Softmax}(X_{t_i}G_{t_i})^{(k)}\right] \in \mathbb{R}^{N\times d_o} \end{aligned} \tag{1}$$

In the shared section, all shared experts E_s and task-specialized experts E_{t_i} are utilized to gather potential features, with a total of $n_s + L \times n_t$ experts. These experts use shared input X_s as their input. Similar to the task-specialized part, a gate fuses shared and task-specialized features. The shared gate network, denoted as G_s, harmonizes the outputs from both shared experts and task-specialized experts across all tasks with weights derived from the shared input X_s. Algorithm 1 described shared and task-specialized parts in the Hybrid Sharing Layer.

$$\begin{aligned} Y_s &= \mathrm{Concat}(Y_{s|s_j}, Y_{s|t_{i,j}}) \in \mathbb{R}^{N\times d_0\times(L\cdot n_t+n_s)} \\ O_s &= \sum_k \left[\sigma(Y_s)^{(k)} \odot \mathrm{Softmax}(X_sG_S)^{(k)})\right] \in \mathbb{R}^{N\times d_0} \end{aligned} \tag{2}$$

It is worth noting that the shared and task-specialized parts receive the outputs from their respective parts in the previous layer as inputs, except the initial layer, which uses an identical input.

4 Experiment

We have performed extensive experiments on two datasets, MS-COCO and PASCAL VOC, to verify the superiority of our model. In accordance with the preceding works, we choose mean average precision as our primary metric. Some experiments also report some secondary metrics, including overall F1-score (OF1) and pre-category F1-score (CF1). Metrics on Top-3 are also reported. The definitions of these metrics are available in the Appendix.

Algorithm 1: Hybrid Sharing Layer Procedure

```
Data: Input to shared experts $X_s$; Input to
      task $t_i$ experts $X_{t_i}$; Shared expert gate
      $G_s$; Task $t_i$ expert gate $G_{t_i}$; Number
      of shared experts $n_s$; Number of
      task-specialized experts per task $n_t$;
      Shared experts $E_{s,(\cdot)}$; Task-specialized
      experts $E_{t_{(\cdot)},(\cdot)}$; Number of labels $L$;
      Activation function $\sigma$
Result: Shared output $O_s$; Task-specialized
        output $O_{t_i}$
$Y_s$ = [ ]
for $i \leftarrow 1$ to $L$ do
    $Y_{t_i}$ = [ ]
end
for $i \leftarrow 1$ to $L$ do
    for $j \leftarrow 1$ to $n_t$ do
        $Y_{s|t_i,j} = X_s E_{t_i,j}$
        $Y_s$.append($Y_{s|_{t_i,j}}$)
        $Y_{t_i|t_i,j} = X_{t_i} E_{t_i,j}$
        $Y_{t_i}$.append($Y_{t_i|t_i,j}$)
    end
end
for $j \leftarrow 1$ to $n_s$ do
    $Y_{s|s_j} = X_s E_{s,j}$
    $Y_s$.append($Y_{s|s_j}$)
    for $i \leftarrow 1$ to $L$ do
        $Y_{t_i|s_j} = X_{t_i} E_{s,j}$
        $Y_{t_i}$.append($Y_{t_i|s_j}$)
    end
end
$A_s \leftarrow \mathrm{Softmax}(G_s X_s)$
$Y_s' \leftarrow \mathrm{Concat}(Y_s)$
$O_s \leftarrow \sum A_s \odot \sigma(Y_s)$
for $i \leftarrow 1$ to $L$ do
    $Y_{t_i}' \leftarrow \mathrm{Concat}(Y_{t_i})$
    $A_{t_i} \leftarrow \mathrm{Softmax}(G_{t_i} X_{t_i})$
    $O_{t_i} \leftarrow \sum A_{t_i} \odot \sigma(Y_{t_i})$
end
```

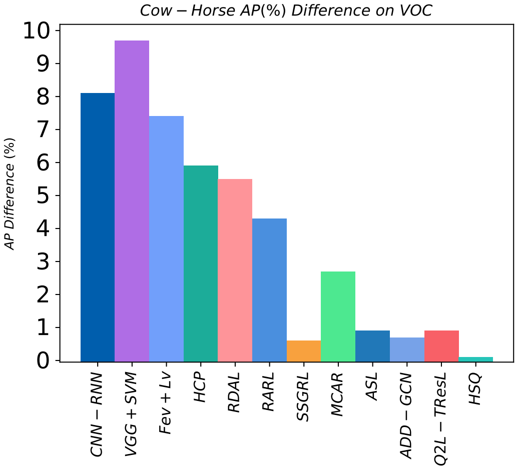

Figure 3: Absolute AP performance difference between cow and horse on VOC dataset in (%)

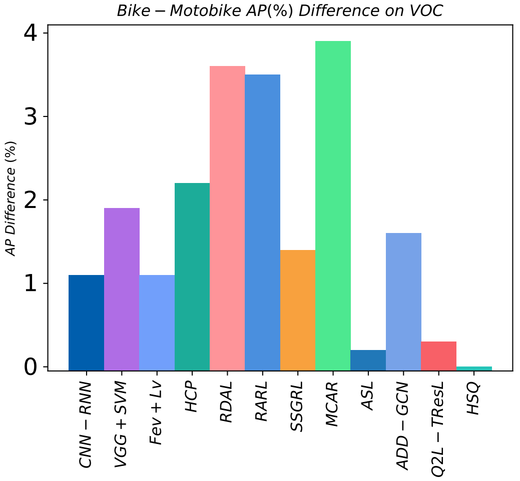

Figure 4: Absolute AP performance difference between bike and motobike on VOC dataset in (%)

4.1 Ablation Study

As shown in Table 1, the number of shared experts greatly influences the performance. We choose ResNet10T as the backbone and Q2L with the same backbone as the baseline. An ablation study is performed on MS-COCO. The input image is fixed at a size of 576 × 576. The proposed model, which includes shared experts (HSQ), outperforms the baseline by 1.3% on mAP, demonstrating that including shared experts facilitates the transfer of information between tasks and mitigates negative transfer. The results also reveal that removing shared experts from the model leads to a considerable drop in performance due to the complete cutoff of sharing information among all tasks, underscoring the importance of sharing features in achieving substantial performance improvements. HSQ-Linear indicates that the hybrid sharing layers of the model are replaced by fully-connected layers with the same depth and dimensions, sharing all information across all labels without discriminating task-specialized information. It is demonstrated that the inclusion of shared experts is a crucial factor in enhancing the performance of the proposed model compared with HSQ-Linear. The findings highlight the potential benefits of incorporating shared experts and can inform the development of future multi-label image classification models.

4.2 Performance on the MS-COCO Dataset

MS-COCO (Lin et al., 2014) is a large dataset of 80 object classes originally for image segmentation and object detection tasks. By extracting object information in annotations, it is also widely used to evaluate various models for multi-label image classification tasks. We test our model on MS-

Table 1: Ablation Study on MS-COCO. n_s, n_t stand for the number of shared experts and task-specialized experts per task, †indicates that it is not available in the original work and we implement it in this paper.

Method	Backbone	Resolution	n_s	n_t	mAP(%)
Q2L-R10T†(Liu et al., 2021a)	ResNet10T	576 × 576	-	-	74.8
HSQ-R10T(Ours)	ResNet10T	576 × 576	0	1	71.5
HSQ-Linear	ResNet10T	576 × 576	-	-	75.7
HSQ-R10T(Ours)	ResNet10T	576 × 576	1	1	76.3
HSQ-R10T(Ours)	ResNet10T	576 × 576	4	1	76.1
HSQ-R10T(Ours)	ResNet10T	576 × 576	16	1	**76.5**

COCO to compare it with previous well-known works and state-of-the-art approaches. Results are shown in Table 2. We use ResNet101 (He et al., 2016) and ConvNeXt (Liu et al., 2022)(CvN) as the backbone and set input resolution to 576 × 576. Those backbones noted with -22k indicate that they are pre-trained on ImageNet-22k. Our HSQ model with CvN as the backbone achieves state-of-the-art performance at an mAP of 92.0%. Among all ResNet101-based approaches, our model outperforms all its counterparts. HSQ-R101 at the resolution of 576 × 576 achieves an mAP of 87.1%. Please note that for this model, we employ two successive Hybrid Sharing Layers of $d_o = 1024, 512$, MLP with one hidden layer of 128 neurons as gate and one of 64 as classifier.

Table 2: Performance (%) on MS-COCO. Bests are in bold. † indicates that it is not available in the original work and we implement it in this paper.

Method	Backbone	Resolution	mAP	All		Top3	
				CF1	OF1	CF1	OF1
SRN (Zhu et al., 2017)	ResNet101	224 × 224	77.1	71.2	75.8	67.4	72.9
ResNet-101 (He et al., 2016)	ResNet101	224 × 224	78.3	72.8	76.8	69.7	73.6
CADM (Chen et al., 2019b)	ResNet101	448 × 448	82.3	77.0	79.6	73.5	76.0
ML-GCN (Chen et al., 2019a)	ResNet101	448 × 448	83.0	78.0	80.3	74.2	76.3
KSSNet (Liu et al., 2018)	ResNet101	448 × 448	83.7	77.2	81.5	-	-
MS-CMA (You et al., 2020)	ResNet101	448 × 448	83.8	78.4	81.0	74.3	77.2
MCAR (Gao and Zhou, 2021)	ResNet101	448 × 448	83.8	78.0	80.3	75.1	76.7
SSGRL (Chen et al., 2019c)	ResNet101	576 × 576	83.8	76.8	79.7	72.7	76.2
C-Trans (Lanchantin et al., 2021a)	ResNet101	576 × 576	85.1	79.9	81.7	76.0	77.6
ADD-GCN (Ye et al., 2020)	ResNet101	576 × 576	85.2	80.1	82.0	75.8	77.9
Q2L-R101 (Liu et al., 2021a)	ResNet101	448 × 448	84.9	79.3	81.5	73.3	75.4
Q2L-R101 (Liu et al., 2021a)	ResNet101	576 × 576	86.5	81.0	82.8	76.5	78.3
SST (Chen et al., 2022)	ResNet101	448 × 448	85.9	80.2	82.2	76.0	77.9
ResNet101+TF (Xu et al., 2022)	ResNet101	576 × 576	85.9	80.3	82.4	-	-
PSD+TF (Xu et al., 2022)	ResNet101	576 × 576	86.7	81.2	82.9	-	-
SCO-DCNN (Zhang et al., 2023)	ResNet101	576 × 576	86.0	79.8	83.0	-	-
HSQ-R101(Ours)	ResNet101	576 × 576	**87.1**	**81.8**	**83.4**	**91.8**	**93.4**
ASL (Ridnik et al., 2021a)	TResNetL	448 × 448	86.6	81.4	81.8	75.1	77.4
TResNetL	TResNetL(22k)	448 × 448	88.4	-	-	-	-
Q2L-TResL (Liu et al., 2021a)	TResNetL	448 × 448	87.3	81.6	83.1	77.0	78.5
Q2L-TResL (Liu et al., 2021a)	TResNetL(22k)	448 × 448	89.2	83.8	84.9	79.0	80.2
MITr-l (Cheng et al., 2022)	MLTr-l(22k)	384 × 384	88.5	83.3	84.9	-	-
Swin-L (Liu et al., 2021b)	Swin-L(22k)	384 × 384	89.6	84.8	86.1	80.0	81.1
CvT-w24 (Wu et al., 2021)	CvT-w24(22k)	384 × 384	90.5	85.4	86.6	80.3	81.3
Q2L-SwinL (Liu et al., 2021a)	Swin-L(22k)	384 × 384	90.5	85.4	86.4	80.5	81.2
Q2L-CvT (Liu et al., 2021a)	CvT-w24(22k)	384 × 384	91.3	85.9	86.8	80.8	81.6
ML-Decoder†(Ridnik et al., 2023)	TResNet-XL(Open Image)	640 × 640	91.2	76.8	76.9	90.8	92.0
HSQ-CvN(Ours)	ConvNeXt(22k)	576 × 576	**92.0**	**86.6**	**87.5**	**94.0**	**95.2**

4.3 Performance on the VOC Dataset

PASCAL-VOC (Everingham et al., 2015) 2007 is also a well-acknowledged dataset for multi-label image classification. It comprises images of 20 classes and is split into train-val and test sets. We follow previous work to train on train-val set and validate on test set on 2007 version. The results of

Table 3: Performance (%) on VOC, in terms of per-label AP and mAP. Bests are in bold.

Methods	aero	bike	bird	boat	bottle	bus	car	cat	chair	cow	mAP
CNN-RNN (Wang et al., 2016)	96.7	83.1	94.2	92.8	61.2	82.1	89.1	94.2	64.2	83.6	84.0
VGG+SVM (Simonyan and Zisserman, 2015)	98.9	95.0	96.8	95.4	69.7	90.4	93.5	96.0	74.2	86.6	89.7
Fev+Lv (Yang et al., 2016)	97.9	97.0	96.6	94.6	73.6	93.9	96.5	95.5	73.7	90.3	90.6
HCP (Wei et al., 2015)	98.6	97.1	98.0	95.6	75.3	94.7	95.8	97.3	73.1	90.2	90.9
RDAL (Wang et al., 2017)	98.6	97.4	96.3	96.2	75.2	92.4	96.5	97.1	76.5	92.0	91.9
RARL (Chen et al., 2018)	98.6	97.1	97.1	95.5	75.6	92.8	96.8	97.3	78.3	92.2	92.0
SSGRL(576) (Chen et al., 2019c)	99.7	98.4	98.0	97.6	85.7	96.2	98.2	98.8	82.0	98.1	95.0
MCAR (Gao and Zhou, 2021)	99.7	99.0	98.5	98.2	85.4	96.9	97.4	98.9	83.7	95.5	94.8
ASL(TResNetL) (Ridnik et al., 2021a)	**99.9**	98.4	98.9	98.7	86.8	98.2	98.7	98.5	83.1	98.3	95.8
ADD-GCN(576) (Ye et al., 2020)	99.8	99.0	98.4	99.0	86.7	98.1	98.5	98.3	85.8	98.3	96.0
Q2L-TResL (Liu et al., 2021a)	**99.9**	98.9	**99.0**	98.4	**87.7**	98.6	**98.8**	**99.1**	84.5	98.3	96.1
HSQ-CvN(22k)	**99.9**	**99.9**	97.2	**99.4**	84.1	**99.1**	98.3	**99.1**	**84.9**	**100.0**	**96.4**

Methods	table	dog	horse	mbike	person	plant	sheep	sofa	train	tv	mAP
CNN-RNN (Wang et al., 2016)	70.0	92.4	91.7	84.2	93.7	59.8	93.2	75.3	99.7	78.6	84.0
VGG+SVM (Simonyan and Zisserman, 2015)	87.8	96.0	96.3	93.1	97.2	70.0	92.1	80.3	98.1	87.0	89.7
Fev+Lv (Yang et al., 2016)	82.8	95.4	97.7	95.9	98.6	77.6	88.7	78.0	98.3	89.0	90.6
HCP (Wei et al., 2015)	80.0	97.3	96.1	94.9	96.3	78.3	94.7	76.2	97.9	91.5	90.9
RDAL (Wang et al., 2017)	87.7	96.8	97.5	93.8	98.5	81.6	93.7	82.8	98.6	89.3	91.9
RARL (Chen et al., 2018)	87.6	96.9	96.5	93.6	98.5	81.6	93.1	83.2	98.5	89.3	92.0
SSGRL(576) (Chen et al., 2019c)	89.7	98.8	98.7	97.0	99.0	86.9	98.1	85.8	99.0	93.7	95.0
MCAR (Gao and Zhou, 2021)	88.8	99.1	98.2	95.1	99.1	84.8	97.1	87.8	98.3	94.8	94.8
ASL(TResNetL) (Ridnik et al., 2021a)	89.5	98.8	99.2	98.6	**99.3**	89.5	99.4	86.8	99.6	95.2	95.8
ADD-GCN(576) (Ye et al., 2020)	88.9	98.8	99.0	97.4	99.2	88.3	98.7	90.7	99.5	97.0	96.0
Q2L-TResL (Liu et al., 2021a)	89.2	**99.2**	99.2	99.2	**99.3**	**90.2**	98.8	88.3	99.5	95.5	96.1
HSQ-CvN(22k)	**91.2**	**99.2**	**99.9**	**99.9**	99.2	88.0	**100.0**	**91.6**	**99.8**	**97.8**	**96.4**

experiments on it are displayed in Table 3. Our model is compared against various established methods and state-of-the-art techniques. Notably, our proposed approach surpasses all its counterparts, achieving an impressive mAP score of 96.4%. The per-class average precision is also presented, with the SOTA performance bolded. Items that improve in comparison with previous works are underscored in the last two rows.

Performance among Labels and Cross-label Comparison Among the 20 available labels, our model exhibits superior performance in 15 of them. Compared to Q2L, another transformer-based model, our model improves 105 pairs of labels, 27 pairs more than Q2L achieved. To provide a visual comparison, we randomly select two labels with moderate performance (i.e., ”table” and ”train”) and illustrate them in Figure 7. In this graph, each dot represents a specific approach, with dots in the upper-right corner indicating better performance. We further explore the performance difference between two pairs of labels with similar semantics, as depicted in Figure 3 and 4. Our method not only outperforms previous work but also exhibits a smaller absolute cross-label performance gap.

Robust Performance across Multiple Image Scales. In addition to previous experiments on MS-COCO, we perform extra experiments on different image scales to verify the performance of our model improves as image resolution decreases in Figure 6. We perform experiments on 576×576, 488×448 and 384×384. Results confirm that our model provides consistent considerable performance as image scale decreases.

4.4 Visualization Result

The proposed model incorporates several gates to harmonize outputs from experts. We verify that different tasks would rely on different experts on PASCAL VOC. Figure 5 depicts the weights of experts' outputs on all 20 tasks and the average load across tasks on a sampled data batch. The last row represents an expert's average load across all tasks. Weights are softmax-activated values of the gate networks' outputs, presented in log scale, along 33 different experts on the X-axis, 32 of which are shared, and the last one is respective task-specialized. A lighter block color indicates an expert with more weight in the final harmonized output. It is evident to note that all tasks focus on different experts. For instance, $E_{s,8}$, $E_{s,30}$, $E_{s,28}$ have the most significant impact on *chair*, *dog* and *horse* respectively. The weight distributions across experts exhibit variations among tasks, indicating that distinct tasks rely on different sets of experts, each extracting distinctive representations, while even average loads on experts show that all experts are engaged during inference.

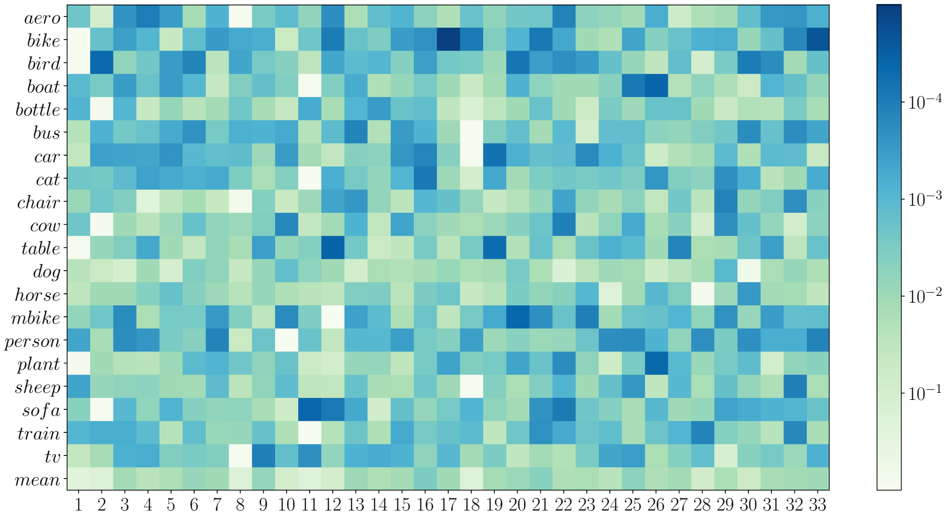

Figure 5: Experts load visualization on 20 labels of VOC2007. Each block indicates a weight for an expert on one task. The first 20 rows represent 20 labels from the VOC dataset, and the last row stands for the average load of experts. The x-axis denotes different experts, where experts 1-32 are shared among all tasks, while expert 33 is task-specific. The color represents weight in log space.

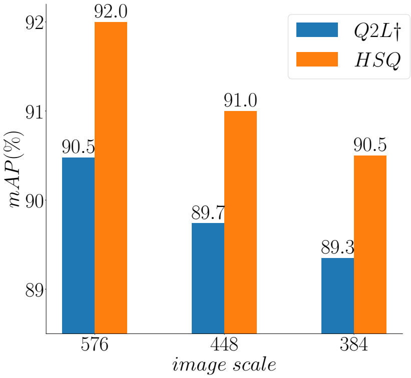

Figure 6: Performance comparison between Q2L (Liu et al., 2021a) and HSQ on MS-COCO with backbone as ConvNext (Liu et al., 2022)(22k)

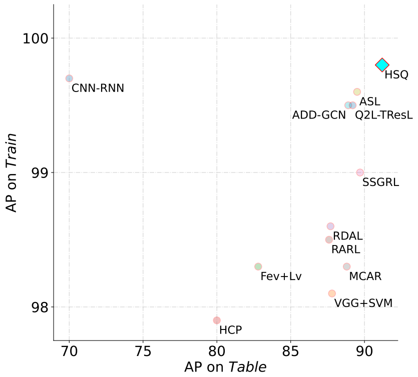

Figure 7: AP on VOC2007 (table and train). The upper-right points in the figure perform better. AP is in %

5 Conclusion

In this paper, regarding MLC as an MTL problem, we introduce HSQ, a transformer-based multi-label image classification model, which is constituted of a feature extraction backbone, query transformer, and Hybrid Sharing Layers that provide evident information sharing among tasks with shared and task-specialized experts leveraging inter- and intra-task information, respectively. Task-specialized experts are organized by respective gate networks, allowing each task to accept correlated information from shared experts independently. Shared experts accept input from all tasks, fusing all potentially useful information. Our model mitigates the negative transfer problem in MLC when formulating it as an MTL problem, where learning several labels jointly may hinder performance improvement. Our experiments demonstrate that HSQ provides a significant improvement on tested datasets. Furthermore, HSQ can simultaneously enhance per-label performance across multiple labels, mitigate performance gap among labels, and effectively handle semantic correlation and heterogeneity.

Reproducibility Statement In this paper, we make efforts to provide detailed information to ensure the reproducibility and completeness of our work. Figure 1 illustrates the architecture of our model. Algorithm 1 and Figure 2 provide a clear overview and procedure for our crucial component, the Hybrid Sharing Layer. Section A.3 in the Appendix describes the hyper-parameters and devices we use, including optimizer, learning rate, *etc*. Section 4.2 and 4.3 describe details on how we prepare our dataset, including version, partitioning strategy, *etc*. The code will be available upon acceptance.

ACKNOWLEDGMENTS

This work is partially supported by the National Natural Science Foundation of China (grant no. 62106101), and the Natural Science Foundation of Jiangsu Province (grant no. BK20210180). This work is also partially supported by the AI & AI for Science Project of Nanjing University.

REFERENCES

Shilong Liu, Lei Zhang, Xiao Yang, Hang Su, and Jun Zhu. Query2label: A simple transformer way to multi-label classification, 2021a.

Tal Ridnik, Gilad Sharir, Avi Ben-Cohen, Emanuel Ben-Baruch, and Asaf Noy. Ml-decoder: Scalable and versatile classification head. In *Proceedings of the IEEE/CVF Winter Conference on Applications of Computer Vision*, pages 32–41, 2023.

Jin Ye, Junjun He, Xiaojiang Peng, Wenhao Wu, and Yu Qiao. Attention-driven dynamic graph convolutional network for multi-label image recognition. In *Computer Vision–ECCV 2020: 16th European Conference, Glasgow, UK, August 23–28, 2020, Proceedings, Part XXI 16*, pages 649–665. Springer, 2020.

Jiaqi Ma, Zhe Zhao, Xinyang Yi, Jilin Chen, Lichan Hong, and Ed H. Chi. Modeling Task Relationships in Multi-task Learning with Multi-gate Mixture-of-Experts. In *Proceedings of the 24th ACM SIGKDD International Conference on Knowledge Discovery & Data Mining*, KDD '18, pages 1930–1939, New York, NY, USA, July 2018. Association for Computing Machinery.

Robert A Jacobs, Michael I Jordan, Steven J Nowlan, and Geoffrey E Hinton. Adaptive mixtures of local experts. *Neural Computation*, 3(1):79–87, 1991.

Feng Zhu, Hongsheng Li, Wanli Ouyang, Nenghai Yu, and Xiaogang Wang. Learning spatial regularization with image-level supervisions for multi-label image classification. In *Proceedings of the IEEE Conference on Computer Vision and Pattern Recognition*, pages 5513–5522, 2017.

Pranav Rajpurkar, Jeremy Irvin, Kaylie Zhu, Brandon Yang, Hershel Mehta, Tony Duan, Daisy Ding, Aarti Bagul, Curtis Langlotz, Katie Shpanskaya, et al. Chexnet: Radiologist-level pneumonia detection on chest x-rays with deep learning. *arXiv preprint arXiv:1711.05225*, 2017.

Gao Huang, Zhuang Liu, Laurens Van Der Maaten, and Kilian Q Weinberger. Densely connected convolutional networks. In *Proceedings of the IEEE conference on computer vision and pattern recognition*, pages 4700–4708, 2017.

Jiang Wang, Yi Yang, Junhua Mao, Zhiheng Huang, Chang Huang, and Wei Xu. Cnn-rnn: A unified framework for multi-label image classification. In *Proceedings of the IEEE Conference on Computer Vision and Pattern Recognition*, pages 2285–2294, 2016.

Zhao-Min Chen, Xiu-Shen Wei, Peng Wang, and Yanwen Guo. Multi-label image recognition with graph convolutional networks. In *Proceedings of the IEEE/CVF conference on Computer Vision and Pattern Recognition*, pages 5177–5186, 2019a.

Jack Lanchantin, Tianlu Wang, Vicente Ordonez, and Yanjun Qi. General multi-label image classification with transformers. In *Proceedings of the IEEE/CVF Conference on Computer Vision and Pattern Recognition*, pages 16478–16488, 2021a.

Sen Wu, Hongyang R Zhang, and Christopher Ré. Understanding and improving information transfer in multi-task learning. In *International Conference on Learning Representations*, 2019.

Rich Caruana. Multitask Learning. *Machine Learning*, 28(1):41–75, July 1997. ISSN 1573-0565.

Long Duong, Trevor Cohn, Steven Bird, and Paul Cook. Low resource dependency parsing: Cross-lingual parameter sharing in a neural network parser. In *Proceedings of the 53rd annual meeting of the Association for Computational Linguistics and the 7th International Joint Conference on Natural Language Processing (volume 2: short papers)*, pages 845–850, 2015.

Yongxin Yang and Timothy Hospedales. Trace norm regularised deep multi-task learning. In *5th International Conference on Learning Representations*, 2017.

Ishan Misra, Abhinav Shrivastava, Abhinav Gupta, and Martial Hebert. Cross-stitch networks for multi-task learning. In *Proceedings of the IEEE conference on computer vision and pattern recognition*, pages 3994–4003, 2016.

Yuan Xie, Shaohan Huang, Tianyu Chen, and Furu Wei. Moec: Mixture of expert clusters. In *Proceedings of the AAAI Conference on Artificial Intelligence*, volume 37, pages 13807–13815, 2023.

Hongyan Tang, Junning Liu, Ming Zhao, and Xudong Gong. Progressive layered extraction (ple): A novel multi-task learning (mtl) model for personalized recommendations. In *Proceedings of the 14th ACM Conference on Recommender Systems*, pages 269–278, 2020.

Noam Shazeer, Azalia Mirhoseini, Krzysztof Maziarz, Andy Davis, Quoc Le, Geoffrey Hinton, and Jeff Dean. Outrageously Large Neural Networks: The Sparsely-Gated Mixture-of-Experts Layer. In *International Conference on Learning Representations*, 2017.

Yanqi Zhou, Tao Lei, Hanxiao Liu, Nan Du, Yanping Huang, Vincent Zhao, Andrew M Dai, Quoc V Le, James Laudon, et al. Mixture-of-experts with expert choice routing. *Advances in Neural Information Processing Systems*, 35:7103–7114, 2022.

Clemens Rosenbaum, Tim Klinger, and Matthew Riemer. Routing networks: Adaptive selection of non-linear functions for multi-task learning. In *International Conference on Learning Representations*, 2018.

Xiaonan Nie, Xupeng Miao, Shijie Cao, Lingxiao Ma, Qibin Liu, Jilong Xue, Youshan Miao, Yi Liu, Zhi Yang, and Bin Cui. Evomoe: An evolutional mixture-of-experts training framework via dense-to-sparse gate. *arXiv preprint arXiv:2112.14397*, 2021.

Simiao Zuo, Xiaodong Liu, Jian Jiao, Young Jin Kim, Hany Hassan, Ruofei Zhang, Tuo Zhao, and Jianfeng Gao. Taming sparsely activated transformer with stochastic experts. *International Conference on Learning Representations*, 2022.

Stephen Roller, Sainbayar Sukhbaatar, Jason Weston, et al. Hash layers for large sparse models. *Advances in Neural Information Processing Systems*, 34:17555–17566, 2021.

Damai Dai, Li Dong, Shuming Ma, Bo Zheng, Zhifang Sui, Baobao Chang, and Furu Wei. Stablemoe: Stable routing strategy for mixture of experts. In *Proceedings of the 60th Annual Meeting of the Association for Computational Linguistics (Volume 1: Long Papers)*, pages 7085–7095, 2022.

William Fedus, Barret Zoph, and Noam Shazeer. Switch transformers: Scaling to trillion parameter models with simple and efficient sparsity. *The Journal of Machine Learning Research*, 23(1): 5232–5270, 2022.

Jack Lanchantin, Tianlu Wang, Vicente Ordonez, and Yanjun Qi. General multi-label image classification with transformers. In *Proceedings of the IEEE/CVF Conference on Computer Vision and Pattern Recognition*, pages 16478–16488, 2021b.

Tsung-Yi Lin, Michael Maire, Serge Belongie, James Hays, Pietro Perona, Deva Ramanan, Piotr Dollár, and C Lawrence Zitnick. Microsoft coco: Common objects in context. In *Computer Vision–ECCV 2014: 13th European Conference, Zurich, Switzerland, September 6-12, 2014, Proceedings, Part V 13*, pages 740–755. Springer, 2014.

Kaiming He, Xiangyu Zhang, Shaoqing Ren, and Jian Sun. Deep residual learning for image recognition. In *Proceedings of the IEEE Conference on Computer Vision and Pattern Recognition*, pages 770–778, 2016.

Zhuang Liu, Hanzi Mao, Chao-Yuan Wu, Christoph Feichtenhofer, Trevor Darrell, and Saining Xie. A convnet for the 2020s. In *Proceedings of the IEEE/CVF Conference on Computer Vision and Pattern Recognition*, pages 11976–11986, 2022.

Zhao-Min Chen, Xiu-Shen Wei, Xin Jin, and Yanwen Guo. Multi-label image recognition with joint class-aware map disentangling and label correlation embedding. In *2019 IEEE International Conference on Multimedia and Expo (ICME)*, pages 622–627. IEEE, 2019b.

Yongcheng Liu, Lu Sheng, Jing Shao, Junjie Yan, Shiming Xiang, and Chunhong Pan. Multi-label image classification via knowledge distillation from weakly-supervised detection. In *Proceedings of the 26th ACM International Conference on Multimedia*, pages 700–708, 2018.

Renchun You, Zhiyao Guo, Lei Cui, Xiang Long, Yingze Bao, and Shilei Wen. Cross-modality attention with semantic graph embedding for multi-label classification. In *Proceedings of the AAAI Conference on Artificial Intelligence*, volume 34, pages 12709–12716, 2020.

Bin-Bin Gao and Hong-Yu Zhou. Learning to discover multi-class attentional regions for multi-label image recognition. *IEEE Transactions on Image Processing*, 30:5920–5932, 2021.

Tianshui Chen, Muxin Xu, Xiaolu Hui, Hefeng Wu, and Liang Lin. Learning semantic-specific graph representation for multi-label image recognition. In *Proceedings of the IEEE/CVF International Conference on Computer Vision*, pages 522–531, 2019c.

Zhao-Min Chen, Quan Cui, Borui Zhao, Renjie Song, Xiaoqin Zhang, and Osamu Yoshie. Sst: Spatial and semantic transformers for multi-label image recognition. *IEEE Transactions on Image Processing*, 31:2570–2583, 2022.

Jiazhi Xu, Sheng Huang, Fengtao Zhou, Luwen Huangfu, Daniel Zeng, and Bo Liu. Boosting multi-label image classification with complementary parallel self-distillation. In Lud De Raedt, editor, *Proceedings of the Thirty-First International Joint Conference on Artificial Intelligence, IJCAI-22*, pages 1495–1501. International Joint Conferences on Artificial Intelligence Organization, 7 2022.

Jialu Zhang, Jianfeng Ren, Qian Zhang, Jiang Liu, and Xudong Jiang. Spatial context-aware object-attentional network for multi-label image classification. *IEEE Transactions on Image Processing*, 2023.

Tal Ridnik, Emanuel Ben-Baruch, Nadav Zamir, Asaf Noy, Itamar Friedman, Matan Protter, and Lihi Zelnik-Manor. Asymmetric loss for multi-label classification. In *Proceedings of the IEEE/CVF International Conference on Computer Vision*, pages 82–91, 2021a.

Xing Cheng, Hezheng Lin, Xiangyu Wu, Dong Shen, Fan Yang, Honglin Liu, and Nian Shi. Mltr: Multi-label classification with transformer. In *2022 IEEE International Conference on Multimedia and Expo (ICME)*, pages 1–6. IEEE, 2022.

Ze Liu, Yutong Lin, Yue Cao, Han Hu, Yixuan Wei, Zheng Zhang, Stephen Lin, and Baining Guo. Swin transformer: Hierarchical vision transformer using shifted windows. In *Proceedings of the IEEE/CVF International Conference on Computer Vision*, pages 10012–10022, 2021b.

Haiping Wu, Bin Xiao, Noel Codella, Mengchen Liu, Xiyang Dai, Lu Yuan, and Lei Zhang. Cvt: Introducing convolutions to vision transformers. In *Proceedings of the IEEE/CVF International Conference on Computer Vision*, pages 22–31, 2021.

Mark Everingham, SM Ali Eslami, Luc Van Gool, Christopher KI Williams, John Winn, and Andrew Zisserman. The pascal visual object classes challenge: A retrospective. *International Journal of Computer Vision*, 111:98–136, 2015.

Karen Simonyan and Andrew Zisserman. Very deep convolutional networks for large-scale image recognition. In *International Conference on Learning Representations*. Computational and Biological Learning Society, 2015.

Hao Yang, Joey Tianyi Zhou, Yu Zhang, Bin-Bin Gao, Jianxin Wu, and Jianfei Cai. Exploit bounding box annotations for multi-label object recognition. In *Proceedings of the IEEE Conference on Computer Vision and Pattern Recognition*, pages 280–288, 2016.

Yunchao Wei, Wei Xia, Min Lin, Junshi Huang, Bingbing Ni, Jian Dong, Yao Zhao, and Shuicheng Yan. Hcp: A flexible cnn framework for multi-label image classification. *IEEE Transactions on Pattern Analysis and Machine Intelligence*, 38(9):1901–1907, 2015.

Zhouxia Wang, Tianshui Chen, Guanbin Li, Ruijia Xu, and Liang Lin. Multi-label image recognition by recurrently discovering attentional regions. In *Proceedings of the IEEE International Conference on Computer Vision*, pages 464–472, 2017.

Tianshui Chen, Zhouxia Wang, Guanbin Li, and Liang Lin. Recurrent attentional reinforcement learning for multi-label image recognition. In *Proceedings of the AAAI conference on Artificial Intelligence*, volume 32, 2018.

Tal Ridnik, Emanuel Ben-Baruch, Asaf Noy, and Lihi Zelnik-Manor. Imagenet-21k pretraining for the masses. *arXiv preprint arXiv:2104.10972*, 2021b.

A Appendix

A.1 Metrics Definition

We here provide the definitions of metrics that are mentioned in our paper.

$$\text{Pre-Category Precision: CP} = \frac{1}{C}\sum_i \frac{N_i^c}{N_i^p}$$

$$\text{Pre-Category Recall: CR} = \frac{1}{C}\sum_i \frac{N_i^c}{N_i^g}$$

$$\text{Pre-Category F1 score: CF1} = \frac{2 \times \text{CP} \times \text{CR}}{\text{CP} + \text{CR}}$$

$$\text{Overall Precision: OP} = \frac{\sum_i N_i^c}{\sum_i N_i^p}$$

$$\text{Overall Recall: OR} = \frac{\sum_i N_i^c}{\sum_i N_i^g}$$

$$\text{Overall F1 score: OF1} = \frac{2 \times \text{OP} \times \text{OR}}{\text{OP} + \text{OR}}$$

where C stands for the number of labels, N_i^c refers to the number of samples that are correctly predicted for the i-th label, N_i^p denotes the number of predicted samples for the i-th label, and N_i^g means the number of ground truth samples for the i-th label.

A.2 FLOPs and #Parameters Details

Model	Backbone	Resolution	FLOPs	#Parameters
Q2L-R10T†(Liu et al., 2021a)	ResNet10T	576	8.4G	14.8M
HSQ ($n_s = 1, n_t = 1$)	ResNet10T	576	8.6G	14.3M
HSQ ($n_s = 16, n_t = 1$)	ResNet10T	576	8.7G	15.5M

A.3 Implementation Details

Unless otherwise stated, the following setting is valid for all experiments. We resize all input images from any dataset to $H_i \times W_i = 576 \times 576$. After a pre-trained backbone with timm, a convolutional layer projection would keep the embedding size $C = C_i = 2048$ as default.

Two layers of mixture-of-expert layers with output embedding dimension $d_o = 64, 16$ are implemented after a transformer with one encoder layer and two decoder layers, followed by a linear layer to make a final prediction.

We train the model for 100 epochs using the Adam optimizer, with weight decay of 1e-2, $(\beta 1, \beta 2)$ = (0.9, 0.9999), and a learning rate of 1e-4. All experiments are run on 4 Tesla V100-SXM2-32GB. The pre-training details of the experiments are provided in parentheses. We, by default, do not train our model on extra data, except if it is otherwise stated. Note that models with -22k indicate that they use a pre-trained backbone on ImageNet22k (Ridnik et al., 2021b). Additionally, experiments marked with † indicate that they have been replicated in this work.